

# Modelling of NBI fast ions and effect of the toroidal ripple in the COMPASS Upgrade tokamak

F. Jaulmes<sup>1</sup>, M. Tomeš<sup>1,2</sup>, M. Imříšek<sup>1,2</sup>, S.Y.F. Cats<sup>3</sup>, L. Karalius<sup>4</sup>, R. Pánek<sup>1</sup>, and the COMPASS team<sup>1</sup>

<sup>1</sup> IPP of the Czech Academy of Science, Za Slovankou 3, CZ-182 00 Prague 8, Czech Republic

<sup>2</sup> Faculty of Mathematics and Physics, Charles University, Prague, Czech Republic.

<sup>3</sup> DIFFER Dutch Institute For Fundamental Energy Research, Eindhoven, The Netherlands

<sup>4</sup> School of Physics and Astronomy - University of Birmingham, Edgbaston, Birmingham, UK

Contact email: jaulmes@ipp.cas.cz

## Introduction

Fast particles are a key component of fusion reactors. In particular, their interaction with turbulent structures and MHD modes can significantly modify the behaviour of the background plasma. The COMPASS Upgrade tokamak [1] will be a tokamak of major radius  $R_0 \sim 0.894\text{m}$  with high-field (Bt=5T) and high-current (Ip=2MA). The machine should be completed by 2022. It will be located in Prague, Czech Republic.

Due to the high particle confinement – high fuelling expected in H-mode in such a tokamak, we anticipate operation at densities of order  $10^{20}\text{m}^{-3}$ [2]. The scaling used to evaluate the H-mode pedestal density is:

$$n_e \approx 0.7 I_p^{0.34} B_t^{0.62} a^{0.95} (R/a)^{0.4}$$

NBI has injection energy of 80keV [-58% of the beam]. This will generate a large population of trapped fast particles in the edge region. We investigate the effect of magnetic Toroidal Field Ripple (TFR) in terms of fast ions losses and distribution in the pedestal and the SOL.

## Transport modelling and equilibrium reconstruction

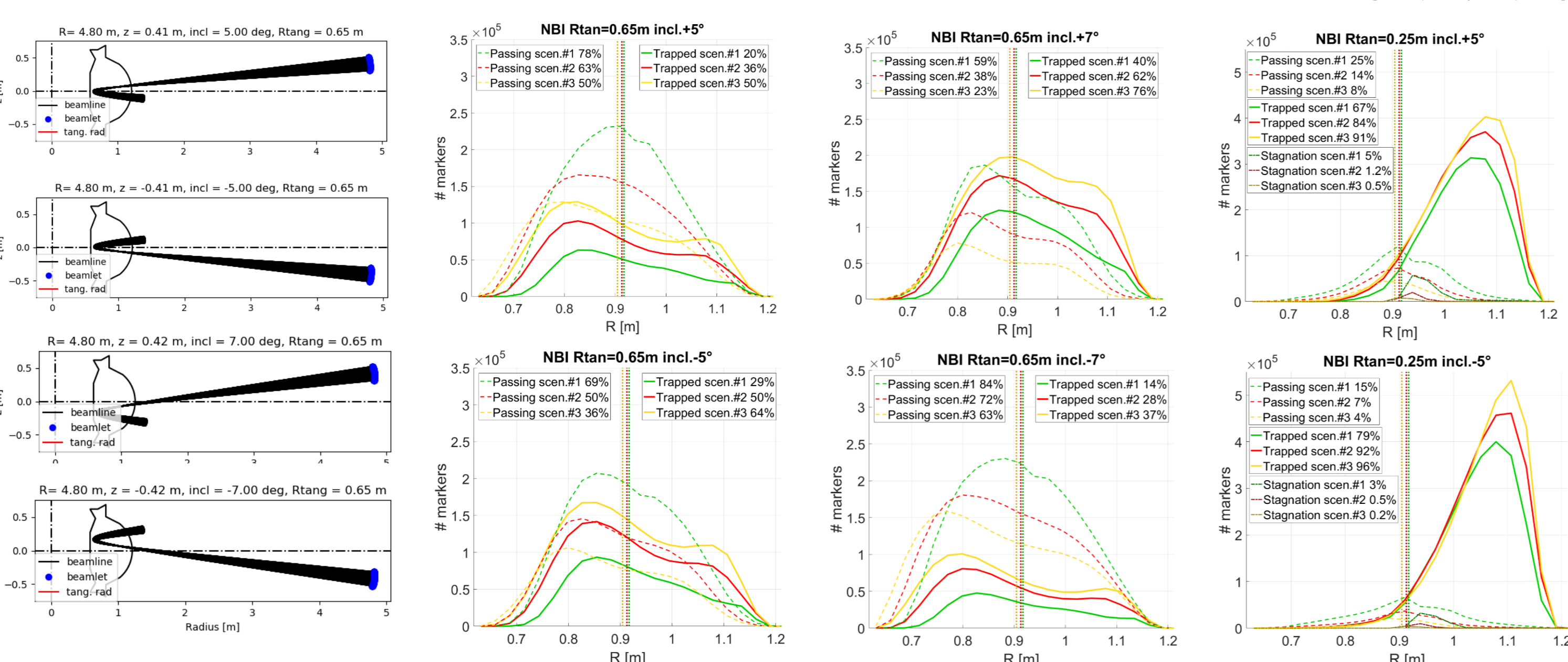
Detailed integrated transport modelling with the METIS code [3] yields density and temperature profiles during the flat-top with 4MW of NBI heating and 2MW of ECRH heating.

Scenario	Bt [T]	Ip [MA]	$\beta$ [%]	$\langle n_e \rangle$ [ $10^{20}\text{m}^{-3}$ ]	$\langle T_e \rangle$ [keV]	$\langle v_{\perp}/3 \rangle$ [ $10^6\text{m/s}$ ]	$T_{e,0}$ [keV]	$T_{e,ped}$ [keV]	$n_{e,ped}$ [ $10^{20}\text{m}^{-3}$ ]	$n_{0,sep}$ [ $10^{14}\text{m}^{-3}$ ]	$d_{SOL}$ [mm]	$L_{inner}$ [m]	$L_{outer}$ [m]	
#1 [3,4]	2.5	0.8	2	1	0.04	40.2	1.3	2.8	0.9	0.43	6	4	20	8.4
#2 [4,4]	4.3	1.4	1.4	1.5	0.03	57.4	1.8	4.2	0.9	0.93	6.4	2	20.2	9.3
#3 [6,4]	5	2	1.4	1.9	0.024	62	1.8	4.3	0.7	1.4	5.5	1	16.4	9.3

The FIESTA code [4] is used to reconstruct the equilibrium using the current distribution from the METIS code. We deliberately choose a large minor radius  $a \sim 0.28\text{m}$  to study potential losses on PFCs.

## NBI geometry and particle distributions

Each NBI box will contain 2 units of 1MW each tilted with an angle (+5° and -5° or +7° and -7°). Tangency radius is at most  $R_{tan} \sim 0.65\text{m}$ . We studied also a configuration with  $R_{tan} \sim 0.25\text{m}$  to consider a low momentum injection. The initial distribution of the birth position & pitch of the NBI particles is given by the BBNBI code [5]. EBdyna\_go code [6] is then used to resolve the orbits.



### → Large fraction of NBI trapped fast particles : orbit width ( $\delta r$ )

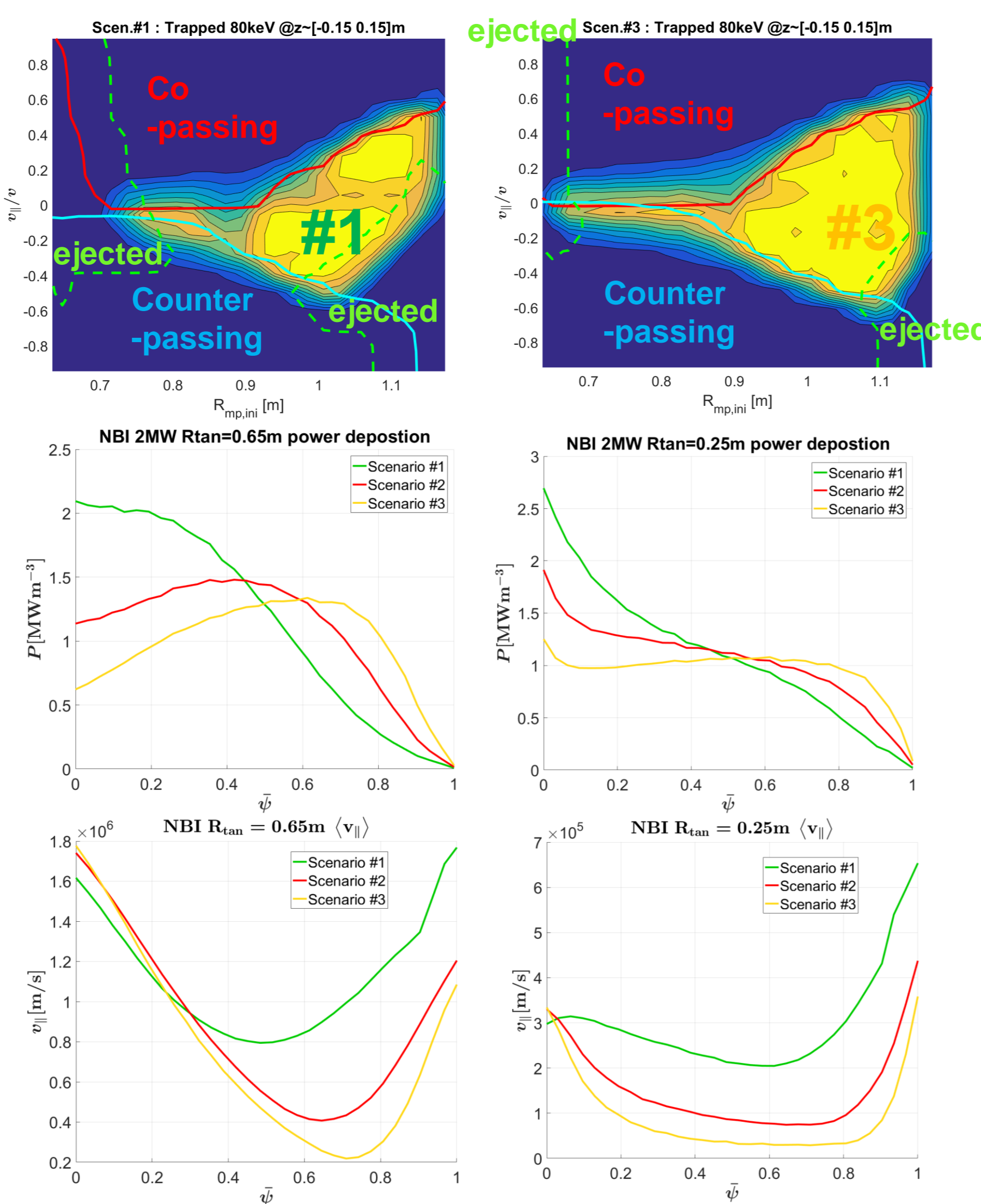
Large trapped population: table indicates: orbit width ( $\delta r$ ) / Larmor radius ( $\rho_L$ ) [in cm]. Promptly ejected particles numbers are negligible.

Scenarios	$R_{tan}$ 0.65m Incl. +/-5°	$R_{tan}$ 0.65m Incl. +/-7°	$R_{tan}$ 0.25m Incl. +/-5°
#1 [3,4]	15.5 / 1.8	15.2 / 1.8	8.6 / 2.2
#2 [4,4]	9 / 1.0	8.4 / 1.1	4.8 / 1.3
#3 [6,4]	6.2 / 0.9	6 / 0.9	3.5 / 1.1

The figures show the trapped population and prompt-loss region (ejected markers) in ( $R_{ini}, v_{\parallel}$ ) space for uniform distribution of 80 keV ions around the mid-plane in scenarios #1 and #3.

## Power given to the plasma and parallel velocity profiles

Assuming each NBI particle slows down to the thermal ion velocity, and neglecting radial transport, we can estimate the power deposited by the combined 2 beams with inclinations +/-5°. We compare the  $R_{tan} \sim 0.65\text{m}$  configuration with  $R_{tan} \sim 0.25\text{m}$ . The latter yields similar heating profiles (even slightly better in the core) with reduced momentum input.



## Modelling of toroidal ripple using a Biot-Savart (BS) solver and Full-orbit Particle trajectories in static 3D-fields

The solution obtained from the Biot-Savart solver is compared with a more elaborate ANSYS calculation and yields similar results.

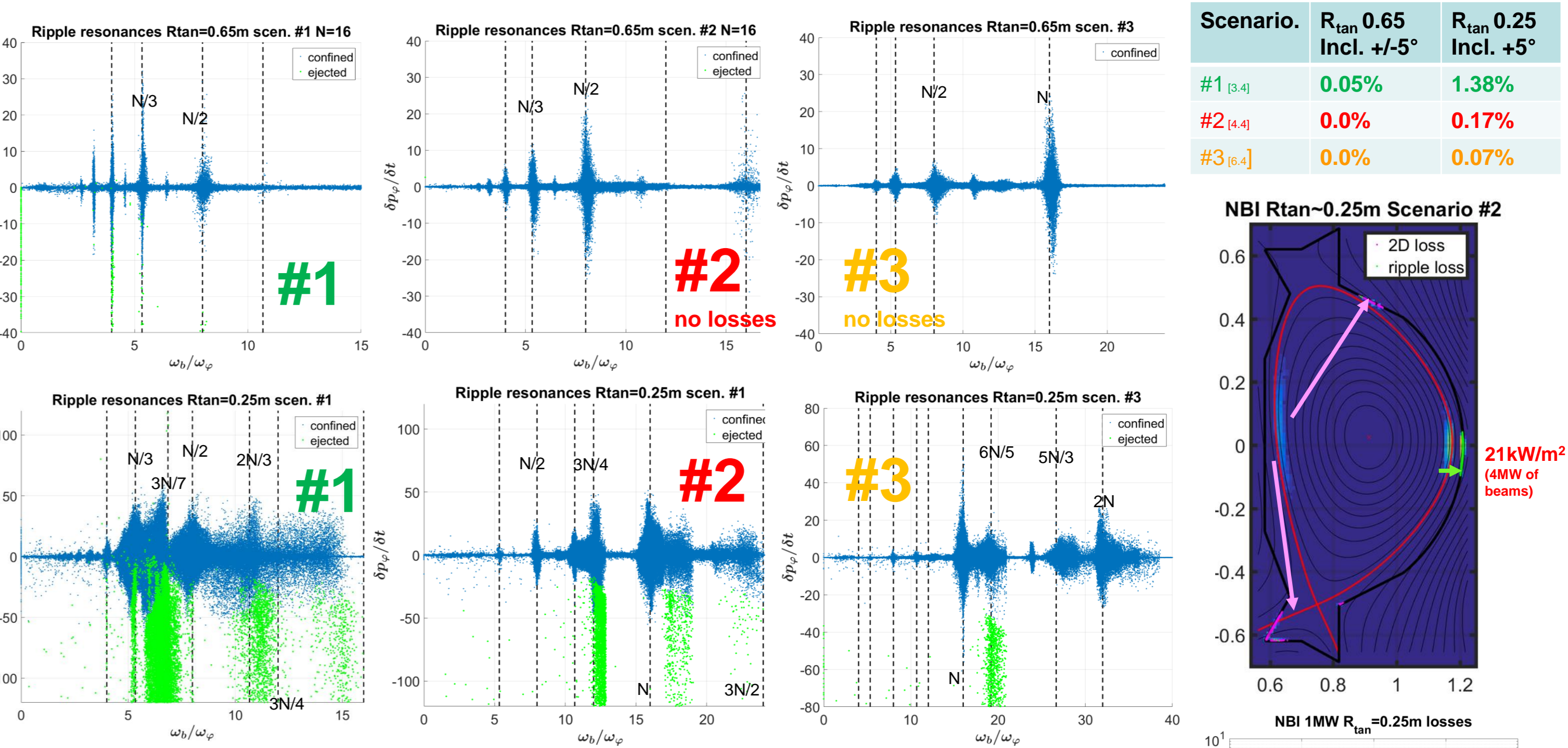
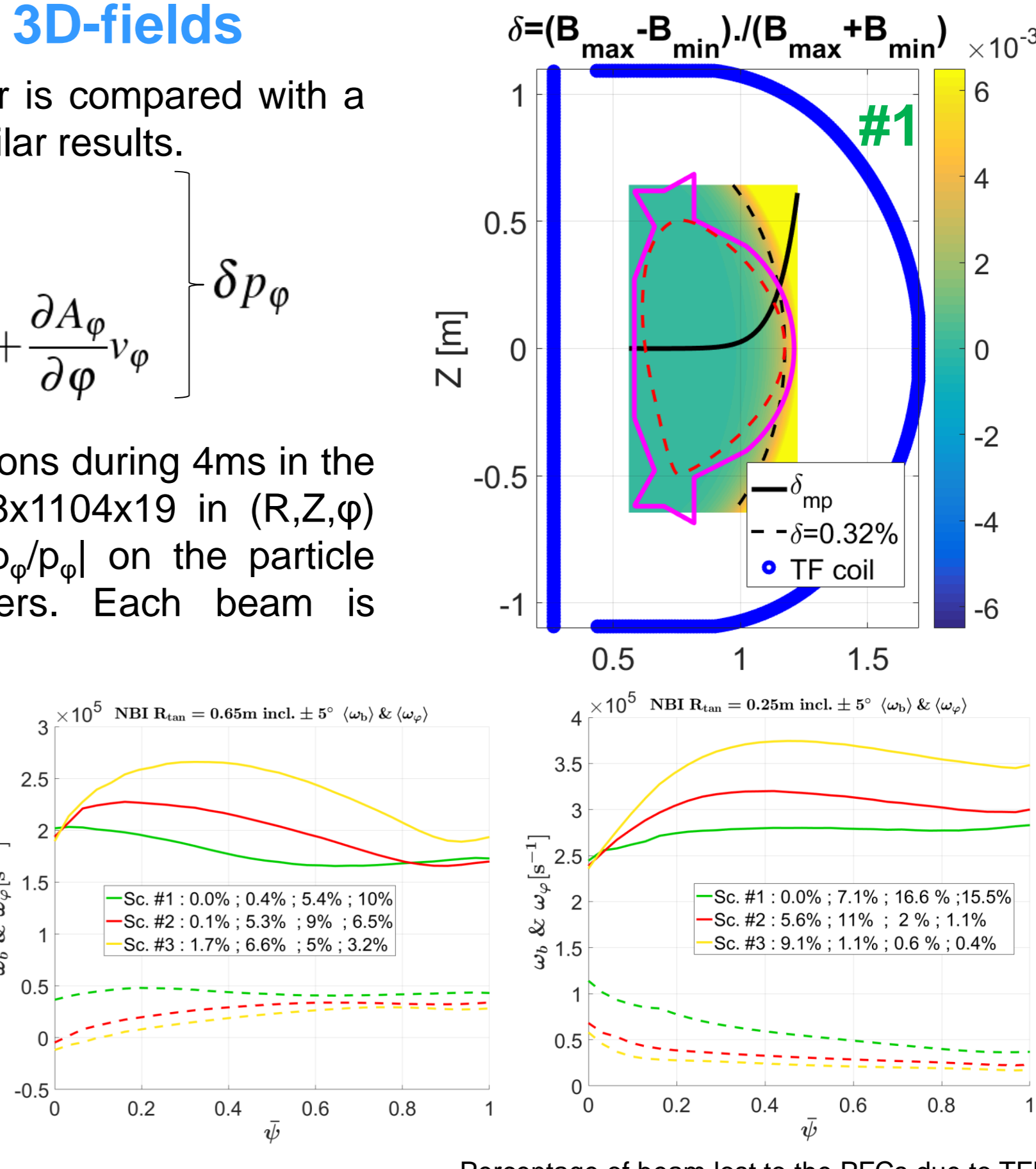
$$\mathbf{B} = \frac{\mu_0}{4\pi} \int_{Coil} \frac{\mathbf{I} \times \mathbf{r}}{r^3} d\mathbf{l} \quad p_{\phi} = mRv_{\phi} - (Z_i e) \psi$$

$$\mathbf{A} = \frac{\mu_0}{4\pi} \int_{Coil} \frac{\mathbf{I}}{r} d\mathbf{l} \quad \frac{1}{Z_i e} \frac{dp_{\phi}}{dt} = \frac{\partial A_R}{\partial \phi} v_R + \frac{\partial A_Z}{\partial \phi} v_Z + \frac{\partial A_{\phi}}{\partial \phi} v_{\phi} \quad \delta p_{\phi}$$

The integrated evolution of the position of NBI D ions during 4ms in the 3D TFR field is done using a grid of size 568x1104x19 in (R,Z,φ) repeated #TF-coils times. The relative error  $|\delta p_{\phi}/p_{\phi}|$  on the particle evolution remains below 0.1% for all markers. Each beam is represented by 3 millions markers.

## Resonance patterns : N=16

Radial transport of trapped fast ions shows a strong correlation to the ratio of the bounce ( $\omega_b$ ) and precession ( $\omega_{\phi}$ ) frequencies [7]. We calculated in the caption of the figures the percentage of particles resonating with [16/1;16/2;16/3;16/4] ratios, for the 3 scenarios, in the more tangential and more perpendicular injection geometries.



The interaction of the NBI particles born from the more perpendicular ( $R_{tan} \sim 0.25\text{m}$ ) injection geometry is much more complex: resonances appear at a larger range of rational fractions of  $N=16$  [2/3 ; 3/7 ; 6/5 ; 3/2 ; 5/3 ; 2] ... The interpretation is not straightforward and might involve resonance overlapping and the larger Larmor radius.

## Sensitivity of losses on the number of TF coils (scenario #1)

Although earlier studies hint at a possible negative impact of the TFR [8] on the overall quality of the confinement (density pump-out), we have assessed the impact of lowering the number of TF coils, since this would allow for better access to the torus for diagnostics and heating systems.

Scenario	$R_{tan}$ 0.65 Incl. +/-5°	$R_{tan}$ 0.25 Incl. +/-5°
#1 [3,4]	0.05%	1.38%
#2 [4,4]	0.0%	0.17%
#3 [6,4]	0.0%	0.07%

### → No large losses are observed lowering TFR to N=14 for the most tangential injection geometry ( $R_{tan} \sim 0.65\text{m}$ )

From the NBI heating perspective there would be no significant impact at higher field to lower the number of TF coils, at least to N=14.

## Population of NBI ions in pedestal and SOL

When we consider the extension of the orbits in the mid-plane, the effect of the TFR is clearly seen on the smaller  $R_{tan} \sim 0.25\text{m}$  injection geometry. Modified gradients of fast particles at the separatrix might change momentum and turbulence in the edge region.

## Conclusions and outlook

A systematic integrated modelling approach (METIS-FIESTA-BBNBI-EBdyna\_go) was developed in order to simulate NBI-born particles in a tokamak. Power deposition and shape of momentum profiles were estimated. Since we neglected collisions, the values need to be further benchmarked against other codes.

The calculations involving the ripple show small loss rate on the wall for  $R_{tan} \sim 0.65\text{m}$  (below  $5\text{kW/m}^2$ ), during 4ms simulations. The configuration with low tangency radius scheme ( $R_{tan} \sim 0.25\text{m}$ ) has the potential to deliver power to the plasma core (scen. #1 and #2) with low momentum input. However, a complex interaction appears between the ripple and deeply trapped ions in the edge region: we anticipate non-negligible losses [scen.#1~120kW/m<sup>2</sup>] and possibly an interaction with the pedestal and SOL.

## References

- [1] R. Pánek et al. Fusion Engineering and Design 123 (2017) 11–16
- [2] F. Rytter et al. 2014 Nucl. Fusion 54 083003
- [3] J.F. Artaud et al. 2018 Nucl. Fusion 58 105001
- [4] G. Cunningham, Fusion Engineering and Design 88 (12) 2013, p. 3238-3247
- [5] O. Asunta et al. Computer Physics Communications 188 (2015) 33–46
- [6] F. Jaulmes et al. 2014 Nucl. Fusion 54 104013
- [7] R.J. Goldston and H.H. Towner, J. Plasma Physics 26, 283 (1981)
- [8] G. Saibene, et al., 22nd IAEA Fusion Energy Conference, Geneva, Switzerland, 13.-18. October, 2008.